SEMI-ACTIVE CONTROL FOR THE SEAT CAR SUSPENSION SYSTEM USING MR ELASTOMER ISOLATOR

Nguyen Quang Du[1]*, Le Cung[2], Nguyen Xuan Bao[1]*

[1] *The University of Danang – University of Technology and Education, Danang, Vietnam*
[2]*The University of Danang – University of Science and Technology, Danang, Vietnam*

*Corresponding authors: nqdu@ute.udn.vn; nxbao@ute.udn.vn

(Received: July 09, 2023; Revised: August 10, 2023; Accepted: September 06, 2023)

Abstract - The suspension system for the car seat is an important part of the vehicle that helps to increase comfort and reduce fatigue. The study of suspension systems using magnetorheological elastomer (MRE) has attracted researchers in recent years. MRE is an elastomer material such as rubber. The modulus of the material can change when a magnetic field is applied. In this study, an MRE-based isolator is first developed for a seat car suspension system. The characteristics of the isolator are investigated under the strength of the magnetic field. Based on Lyapunov theory and constraint force, the semi-active controller is then designed. Numerical simulations for the car seat dynamics system show that the developed isolator can reduce vibrations more when compared with the passive approach in the case of bump and random excitations. The results show significant potential for its application in vehicle seat vibration control.

Key words - Seat car suspension; MR elastomer; semi-active control.

1. Introduction

Magnetorheological elastomer (MRE) is a smart material that has been of interest to many researchers recently [1, 2]. Numerical models have been developed for MRE [3-5]. The material's elastic properties can be adjusted under a magnetic field strength. MRE is suitable for many applications, including vibration reduction, energy absorption, and shock absorption. There is very little research on this device for suspension.

A semi-active suspension system is a type of suspension system that has attracted much attention in recent years. Unlike a fixed passive suspension system that cannot be adjusted in real-time, a semi-active suspension system uses control units to adjust the suspension stiffness and damping rates. A semi-active suspension system can adjust the stiffness or damping coefficient in real time based on road conditions, vehicle speed, and driver inputs. The system provides a smoother and more comfortable ride while improving handling and stability. They can also adapt to changing road conditions and provide a more dynamic driving experience. However, they are more complex and expensive than passive suspension systems and require a semi-active controller. A semi-active seat car suspension system is a type of suspension system that is designed to improve ride comfort and reduce the impact of vibrations on the driver and passengers. The use of MRE material for the semi-active suspension of car seats is a novelty expected to provide high efficiency.

The suspension system needs a semi-active controller to work efficiently. The skyhook is a common type of semi-active control algorithm [6-9]. The algorithm is effective in reducing vibration. Other algorithms have also been developed, such as an adaptive sliding mode controller [10, 11, 14], an adaptive fuzzy controller [12, 13], clipped-optimal control algorithm [14]. Adaptive semi-active control has also been of interest in recent years [16, 17]. In general, semi-active control algorithms are designed to provide an optimal balance between performance and energy efficiency and can be customized to suit different applications and control objectives.

Semi-active control is an effective technique to improve the performance of car seat suspension. MR elastomer isolators have emerged as a promising technology for implementing this approach. These isolators use a magnetic rheological MR elastomer that changes its rheological properties in response to an external magnetic field. By controlling the strength of the magnetic field, it is possible to adjust the stiffness of the isolator in real-time. The isolator allows the seat suspension to adapt to different road conditions and improves driving comfort and handling. The use of MRE-based isolators in semi-active suspension control systems shows excellent potential in enhancing the performance and safety of car seat suspension systems.

2. Development of MRE-Based Isolator

2.1. Fabrication of MRE

Magnetic rheological elastomers (MR) are smart materials that can deform or reshape when exposed to an external magnetic field. They are made of an elastic matrix filled with iron particles or other ferromagnetic materials. The particles are suspended in the matrix by a network of cross-linked molecules. When the material is exposed to a magnetic field, the particles are magnetized and interact, causing the elastomer to become stiffer and stiffer. The stiffness value can be controlled by varying the strength of the magnetic field.

The fabrication process of MRE is shown in Figure 1. Room-temperature vulcanized silicone rubber (RTV) and silicone oil were selected as the matrix. The average diameter of carbonyl iron particles is about 5 mm (BASF Company). The volume fraction ratios of silicone rubber, iron particles, and silicone oil in the material are 68%, 30%, and 2%. The carbonyl iron particles are soaked in silicone oil and mixed with RTV silicone rubber. This mixture is put into a vacuum chamber to remove air bubbles inside, and then the mixture is poured into the mold and cured for about 24 hours at room temperature.

During vulcanization, a magnetic field (500 mT) passes through the material to create anisotropic MRE samples.

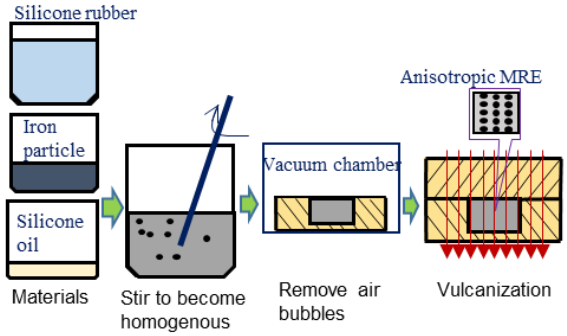

Figure 1. *MRE fabrication process*

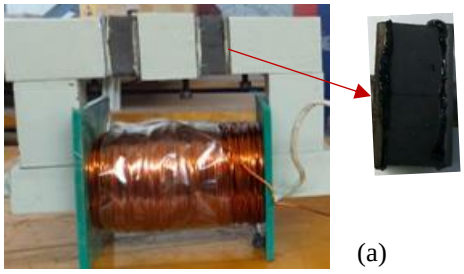

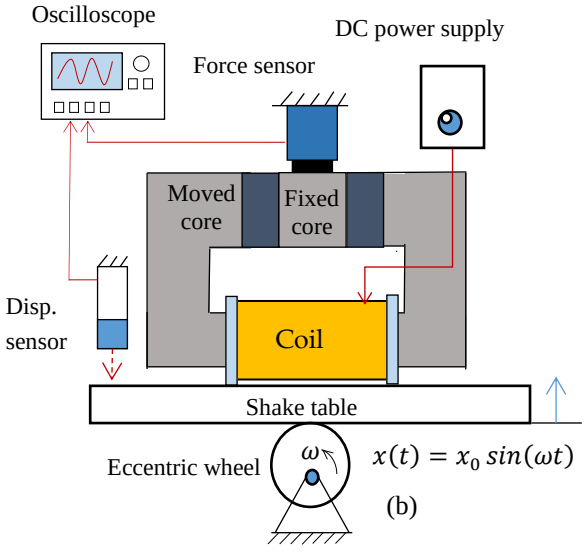

Figure 2. *Mechanical measurement diagram for MRE-based isolator: (a) MRE-based isolator, (b) mechanical measurement diagram*

2.2. Development of an MRE-based isolator

MRE-based isolators are devices that use MRE to provide vibration isolation and damping. An effective MRE isolator requires an optimizations and control strategy considering several factors. The optimization process involves selecting the appropriate MRE material and designing the isolator's geometry to achieve the desired performance. The material properties of the MREs, such as the magnetic susceptibility and viscosity, must be carefully chosen to provide the required stiffness, damping, and isolation properties. The geometry of the isolator must also be designed to provide the required vibration isolation and damping while maintaining a compact size and low weight. The manufacturing process involves preparing the MREs and assembling the isolator. The MREs are typically made by mixing magnetic particles into a polymer matrix, then cured. The resulting MRE material is then cut or molded into the desired shape for the isolator.

The proposed one-fifth scale MRE-based isolator for the driver's seat was developed, as shown in Figure 2(a). The relationship between the magnetic field and current of the coil is described by Ampère's law and the right-hand rule. Electric current is applied to the coil that generates a magnetic field in the core. The equation for the magnetic field strength inside a solenoid (coil) with an iron core becomes, $B = \mu.n.I$, where n is the number of turns per unit length of the coil, $n = N/l$, with N and l are the number of turns and the length of coil, respectively (N=600, l=0.1), $I \in [0, 4\text{A}]$ is the current passing through the coil, and μ represents the magnetic permeability of the iron core ($\mu = 6.3 \times 10^{-3}$ H/m).

The isolator includes a moved core, fixed core, coil, and MRE material. The coils, the core of which form the electromagnet, are used to generate different magnetic fields. In this design, the isolator acts as a variable spring. The applied current can be controlled by electrical power to regulate the strength of the magnetic field. As a result, the modulus of the MRE can be controlled in real-time, i.e., the spring stiffness can be adjusted to suit special needs.

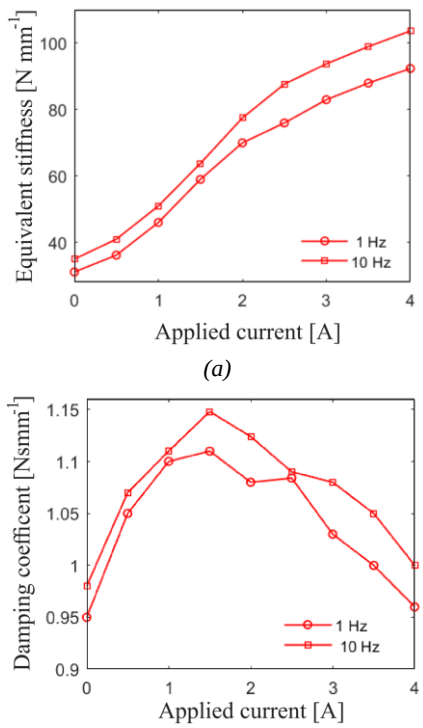

Figure 3. *Mechanical properties of MRE dampers: (a) stiffness, (b) damping coefficient*

Experiments were conducted on the system illustrated in Figure 2(b). The force-displacement responses of the MRE-based device were measured with a load cell (PCB PIEZOTRONICS 208C02) and a laser displacement sensor (KEYENCE LB- 02). Responses were processed using a Fast Fourier Transform (FFT) spectrum analyzer (TEKTRONIX MDO3022). Different flux densities are

provided using a direct current (DC) power supply (KIKUSUI PMC-5AS). Shear deformation is performed sinuously by an eccentric wheel. The rotational speed of the wheel represents the shear frequency. The eccentricity represents the shear amplitude.

Stiffness is calculated in $K = F_0/x_0$ where x_0 is the displacement amplitude, and F_0 is the force amplitude. Damping coefficient is calculated in, $C = \Delta E/(F_0 x_0)$ where ΔE is the dissipated energy which is calculated by the area of the response loop. The properties of the MRE isolator are shown in Figure 3. The stiffness of the MRE increases steadily with the magnetic field (current). The increase of more than twofold when changing the applied current from 0 A to 4 A. Viscosity coefficient does not change significantly with changing amperage. Experimental results show that MRE is expected for intelligent vibration systems. It implies that the MRE can act as a variable damping and stiffness material.

We use the model method of determining parameters developed by Nguyen et al. [8]. The model consists of three parts consists of smooth Coulomb friction, a standard linear solid model, and a variable stiffness spring, connected in parallel,

$$F_{MRE} = F_v + F_m + F_f, \quad (1)$$

Where, $F_v = K_1 x + C\dot{x}_1 = K_2(x - x_1)$ represent the basic viscosity of the material; $F_m = K_m x$ representing the variable stiffness under a magnetic field; F_f is the Coulomb friction model representing the hysteresis of the material and depends on the maximum frictional force F_{max}.

The parameters of the model are determined $xK_1 = 30$ N/mm, $K_2 = 20$ N/mm, $C = 0.05$ Ns/mm,$x_2 = 0.9$. The values F_{fmax} and K_m depend on the applied current and are determined based on experiments under different amperage levels, $F_{fmax}(I)$ is the response force value at $x = 0$, where $K_m(I) = (F_0(I) - F_0(0))/x_0$, where $F_0(I)$ is the response force amplitude when a applied current (I) is applied, $F_0(0)$ is the force amplitude response when current isn't applied. The equations below are based on the linear regression method, $F_{f\,max} = -0.4I^2 + 5I + 5$, and $K_m = -0.6I^2 + 20I$. The model shows the material's properties well when varying the amperage applied, as shown in Figure 4(b). The shear strain is sinuous function with a frequency of 1 Hz; the shear amplitude is set at 0.4 mm, applied current increases gradually from 0-4A. The force amplitude (F_0) and dynamic stiffness values (K_0) of the MRE-based isolator are shown in Table 1. Values measured at 1 Hz, stiffness determined $K_0 = F_0/x_0$, nominal force amplitude values taken when no current is applied, and with a factor of one, values in the brackets show the rate of increase in force amplitude when current is applied. The table shows that the force amplitude (stiffness) increases almost 2.8 times when a current of 4 A is applied. The amplitude increases rapidly when the current increases from 0 A to 3 A and increases slowly when the applied current is increased from 3 A to 4 A. The amplitude reaches saturation when the applied current is above 4 A.

Besides, the area of the response loop also increases significantly, which proves that the material's hysteresis depends on the magnetic field. The stiffness of the MRE increases with the increase of applied current. When the current reaches 4 A, the rheological effect reaches a plateau. The MRE achieves a phase of magnetic saturation. The damping coefficient C does not change significantly, reaching the maximum value when the current is about 2 A, as shown in Figure 3(b). The dynamic stiffness and the damping coefficient increase as the excitation frequency increases and are highly frequency dependent.

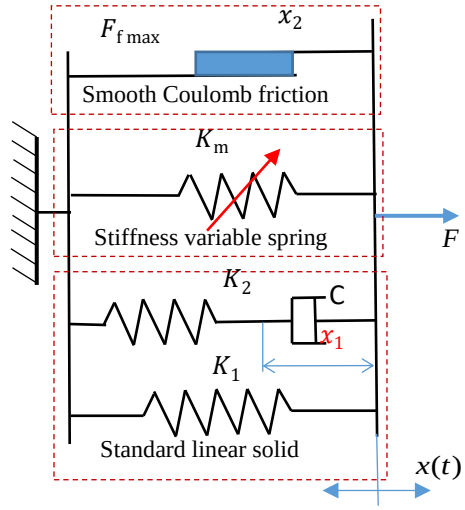

(a)

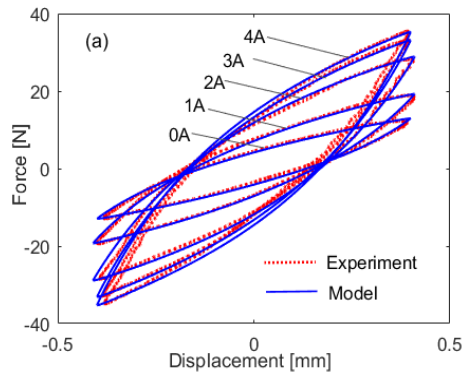

(b)

Figure 4. *Numerical MRE-based isolator model [8]: (a) the model, (b) the model response*

Table 1. *The force amplitude and dynamic stiffness values of MRE-Based isolator*

Applied current (A)	The force amplitude F_0 (N)	Dynamic stiffness, $K_0 = F_0/x_0$ (N/mm)
0 (A)	13 (1)	32
1 (A)	19 (1.5)	47
2 (A)	27 (2.1)	68
3 (A)	33 (2.5)	82
4 (A)	36 (2.8)	90

3. Semi-active control for car seat suspension

The semi-active control strategy involves controlling the magnetic field applied (or applied current) to the MRE material to achieve the desired stiffness and damping

properties. It can be done using a feedback control system that measures the system's vibration and adjusts the magnetic field accordingly. The semi-active control strategy must be designed to provide the required isolation and damping while minimizing power consumption and maintaining stability.

3.1. Dynamic model

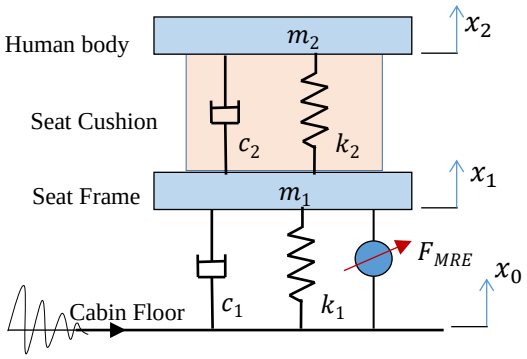

Figure 5. *Seat suspension model using MRE-based isolator with human body*

Figure 5 displays the seat car suspension system, which includes an MRE-based isolator (F_{MRE}), seat frame, and human body. For the simple dynamics model, the vertical motion of the vehicle is considered. The excitation input is transmitted to the cabin floor. The MRE-based isolator response value is five times as large as the developed isolator in Section 2.

The equation of motion of the seat car suspension with the human body is as follows.

$$m_1\ddot{x}_1 + c_1(\dot{x}_1 - \dot{x}_0) + k_1(x_1 - x_0) + c_2(\dot{x}_1 - \dot{x}_2) + k_2(x_1 - x_2) = F_{MRE} \quad (2)$$

$$m_2\ddot{x}_2 + c_2(\dot{x}_2 - \dot{x}_1) + k_2(x_2 - x_1) = 0 \quad (3)$$

Where, m_1, k_1,and c_1 are the mass, stiffness, and damping coefficient of seat frame, respectively; m_2, k_2, and c_1 are the mass, stiffness, damping coefficient of human body, respectively.

3.2. Adaptive active control for the suspension system

Assume the suspension uses an active isolator with control force F_c instead of a semi-active MRE-based isolator (F_{MRE}). The active controller F_c can satisfy the requirements of the control algorithm. The dynamic equation of the seat frame Eq. (2) using an active isolator rewritten as follows,

$$\ddot{x}_1 = \rho F_c + \vartheta x + g \quad (4)$$

Where, ϑ is the parameter vector, and x is the corresponding repressor vector,

$$\rho = \frac{1}{m_1}, \quad \vartheta = \left[-\frac{c_1 + c_2}{m_1} \quad \frac{c_2}{m_1} \quad -\frac{k_1 + k_2}{m_1} \quad \frac{k_2}{m_1}\right],$$

$$x = [\dot{x}_1 \quad \dot{x}_2 \quad x_1 \quad x_2]^T.$$

The cabin signals are measured, the component related to the excitation from the cabin (g). Assume that Γ is a known component and satisfies,

$$g = k_1 x_0 + c_1 \dot{x}_0, \ |g|_{max} \le \Gamma. \quad (5)$$

The designed sliding surface ensures the system's state converges and remains on this surface, achieves the desired response. In this study, a basic form of the sliding surface is as follows, depending only on a single scalar parameter, $\lambda > 0$. The Sliding surface S is define as,

$$S = \dot{x}_1 + \lambda x_1 = 0. \quad (6)$$

The dynamic equation of the system is rewritten terms of S,

$$\dot{S} = \rho F_c + \vartheta x + \lambda \dot{x} + g \quad (7)$$

Parameters of the model ρ and ϑ are uncertain values. Suppose $\hat{\rho}$ and $\hat{\vartheta}$ represent the estimated values of ρ and ϑ, respectively, $\tilde{\rho} = \hat{\rho} - \rho$ and $\tilde{\vartheta} = \hat{\vartheta} - \vartheta$ denote the estimation errors.

The proposed active control algorithm is as follows,

$$F_c = -(\hat{\rho})^{-1}\left[kS + \hat{\vartheta}x + \lambda\dot{x} + \Gamma \text{sign}(S)\right] \quad (8)$$

The adaptive algorithm is proposed as,

$$\dot{\hat{\rho}} = \sigma_1 \frac{1}{\hat{\rho}} S\left(kS + \hat{\vartheta}x + \lambda\dot{x} + \Gamma \text{sign}(S)\right) \quad (9a)$$

$$\dot{\hat{\vartheta}} = -\sigma_2 S x^T \quad (9b)$$

Theorem: Consider the closed-loop dynamic system of the motion as Eq. (7), control algorithm represented by Eq. (8), and adaptive algorithm denoted by Eqs. (9). The gain k, σ_1, and σ_2, are all positive constants, and Γ is known in advance then

1) $x(t) \to 0$ as $t \to \infty$.

2) All signals must be bounded for $\forall t \ge 0$

Lyapunov candidate is positive definite $V(S, \tilde{\rho}, \tilde{\vartheta}) > 0, \forall S, \tilde{\rho}, \tilde{\vartheta} \in R$. The control algorithm and adaptive algorithms ensure that the derivative of Lyapunov is always negative $\dot{V}(S, \tilde{\rho}, \tilde{\vartheta}) > 0, \forall S, \tilde{\rho}, \tilde{\vartheta}$, then the variables of the Lyapunov function will be asymptotic and stable at zero ($S, \tilde{\rho}, \tilde{\vartheta} \to 0$).

Proof: Lyapunov candidate is chosen as,

$$V(S, \tilde{\rho}, \tilde{\vartheta}) = \frac{1}{2}S^2 + \frac{1}{2\sigma_1}\tilde{\rho}^2 + \frac{1}{2\sigma_2}\tilde{\vartheta}\tilde{\vartheta}^T. \quad (10)$$

The Lyapunov derivative is defined as follows,

$$\dot{V}(S, \tilde{\rho}, \tilde{\vartheta}) = S\dot{S} + \tilde{\rho}\dot{\tilde{\rho}} + \tilde{\vartheta}\dot{\tilde{\vartheta}}^T$$

$$= S(\rho F_c + \vartheta x + \lambda\dot{x} + g) + \tilde{\rho}\dot{\tilde{\rho}} + \tilde{\vartheta}\dot{\tilde{\vartheta}}^T$$

$$= S\left(-\frac{(\hat{\rho} - \tilde{\rho})}{\hat{\rho}}\left(kS + \hat{\vartheta}x + \lambda\dot{x} + \Gamma \text{sign}(S)\right) + \vartheta x + \lambda\dot{x} + g\right) + \frac{1}{\sigma_1}\tilde{\rho}\dot{\tilde{\rho}} + \frac{1}{\sigma_2}\tilde{\vartheta}\dot{\tilde{\vartheta}}^T$$

$$= -kS^2 + S\left(-\left(\hat{\vartheta}x + \lambda\dot{x} + \Gamma \text{sign}(S)\right) + \vartheta x + \lambda\dot{x} + g\right) + \frac{1}{\sigma_2}\tilde{\vartheta}\dot{\tilde{\vartheta}}^T + \frac{1}{\sigma_1}\tilde{\rho}\dot{\tilde{\rho}} - \frac{\tilde{\rho}}{\hat{\rho}}S\left(kS + \hat{\vartheta}x + \lambda\dot{x} + g\right)$$

$$= -kS^2 + \left(\vartheta - \hat{\vartheta}\right)Sx + \frac{1}{\sigma_2}\tilde{\vartheta}\dot{\tilde{\vartheta}}^T - \Gamma \text{sign}(S)S + g + \frac{1}{\sigma_1}\tilde{\rho}\dot{\tilde{\rho}} - \frac{\tilde{\rho}}{\hat{\rho}}S\left(kS + \hat{\vartheta}x + \lambda\dot{x} + \text{sign}(S)\right)$$

$$\leq -kS^2 + \tilde{\vartheta}\left(Sx + \frac{1}{\sigma_2}\dot{\hat{\vartheta}}^T\right) + \tilde{\rho}\left[\frac{1}{\sigma_1}\dot{\hat{\rho}} - \frac{1}{\hat{\rho}}S\left(kS + \hat{\vartheta}x + \lambda\dot{x} + \text{sign}(S)\right)\right] \quad (11)$$

It should be noted that $|g|_{max} \leq \Gamma$ and therefore $-\Gamma\text{sign}(S)S + gS \leq 0$. By substituting Eqs. (9a)–(9b) into Eq. (11), the Lyapunov derivative is achieved as,

$$\dot{V}(t) \leq -kS^2 \quad (12)$$

The Lyapunov function $V(t)$ is a nonincreasing function. As the values of $S, \tilde{\rho}$, and $\tilde{\vartheta}$ are bounded, the estimated values of $\hat{\rho}$ and $\hat{\vartheta}$ are also bounded by definition.

According to Barbalat's lemma, the system implies that the displacement $x(t)$ will converge to zero asymptotically

$$\lim_{t\to\infty} S(t) = 0 \text{ and } \lim_{t\to\infty}(x_1(t),\ \dot{x}_1(t)) = 0. \quad (13)$$

3.3. Semi-active control

The suspension using an MRE-based isolator is a semi-active system. The force response of the isolator (F_{MRE}) does not meet the ideal control force, as shown in equation (5). Furthermore, the actual control signal for the isolator is the applied current (I). The clipping-optimal control algorithm for the system is shown below. The controller is divided into two stages: an ideal active controller and a passive controller, in which an "on-off" algorithm turns on the control variable. The following clipped on-off algorithm is used to determine the current from the above adaptive control algorithm,

$$I = I_{max}H((F_c - F_{MRE})F_{MRE}) \quad (14)$$

Where, I is the control current for the MRE damper, $H(.)$ is the Heaviside function, I_{max} is the maximum applied current value to achieve the maximum stiffness (I_{max}= 4 A), F_c is the value ideal control force value as designed in Eq. (8), F_{MRE} is the force value measured on the MRE-base isolator. In the simulation, F_{MRE} is calculated by using the model [8].

The control algorithm (Eq. 14) is divided into two stages as,

$$I = \begin{cases} I_{max} & if\ (F_c\text{-}F_{MRE})F_{MRE} > 0 \\ 0 & if\ (F_c\text{-}F_{MRE})F_{MRE} \leq 0 \end{cases} \quad (15)$$

4. Simulation Results

Simulations are performed to confirm the effectiveness of the proposed control. The parameters are listed in Table 2, which are studied from benchmark seat car suspension [19, 20]. We use Matlab version 2018 to solve the kinematic Eqs. (2, 3). The isolator force is calculated by Eq. (1), and the applied current is determined by Eq. (14). The differential equations are solved using the ode23 Matlab function. The random and bump excitation is used to evaluate the suspension's efficiency using the MRE-based isolator.

The simulation results are presented in Figures 6 and 7. The results of the proposed system are compared with the results of the passive system and the sky-hook controller [15]. Figure 6 shows the displacement capacity of the body for random excitation. The proposed controller reduces mass vibrations (m_2) significantly compared to the passive and sky-hook methods. Figure 7 shows that the human body has been isolated under the bump excitation and the displacement reduced considerably. The root mean square (RMS), which is determined by Eq. (15). RMS was reduced by 41% and 47%, respectively, compared to the case of passive system.

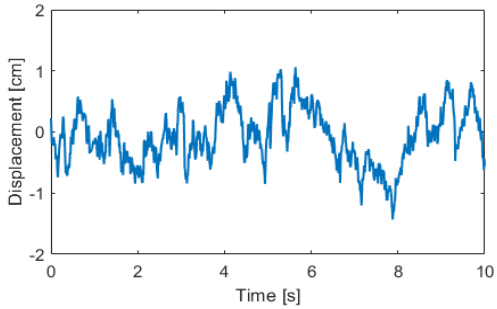

(a)

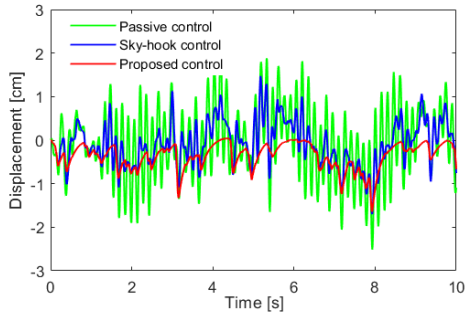

(b)

Figure 6. *Body-human displacement response to random excitation: (a) random excitation profin and (b) body-human response*

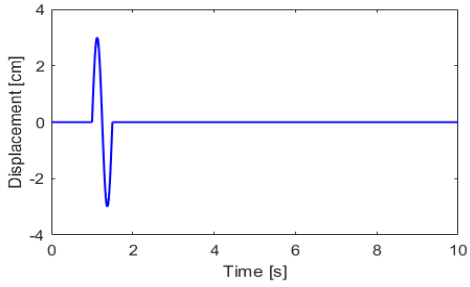

(a)

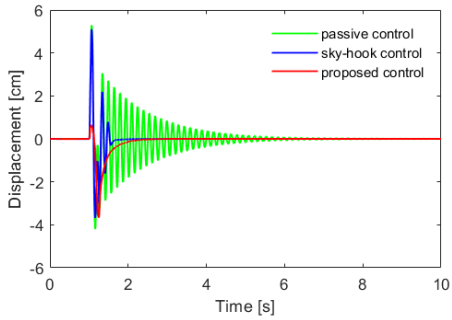

(b)

Figure 7. *Body-human displacement response to bump excitation: (a) bump excitation profin and (b) body-human response*

The root mean square (RMS) is the average of the squares of a group of values and is calculated as follows,

$$\text{RMS}=\sqrt{\frac{1}{n}\sum_{i} x_i^2}, \quad (16)$$

Where, n is number sample of data measurement; x_i is value of the i'th sample.

Table 2. *Parameters of the seat car suspension system*

Mass (kg)	***Stiffness*** (N/m)	***Damping coefficient*** (Ns/m)
m_2 50	k_2 44100	c_2 441
m_1 26	k_1 17085	c_1 1000

In the simulation, the simulated isolator model has a force magnitude five times larger than the model investigated in Section 2 used to simulate the seat car suspension system. The control force value is adjustable from 62 N to 160 N, the same value as the semi-active seat car suspension system [18]. It makes experimental sense since the parallel connection but five MRE isolators can guarantee the stiffness response for the full-scale car seat ratio. However, a full-scale MRE isolator may be needed in practical applications to accomplish the intended tasks. According to the applicable requirements, the size of the MRE isolator can be estimated. However, it is essential to note that developing an effective MRE isolator still requires further research, including optimization, manufacturing, and control strategy development.

5. Conclusion

This study aims to investigate the seat car suspension system using MRE-based isolator by a dynamic model and a semi-active controller. The main achievements of this study are summarized as follows,

1) Development of MRE-based isolator using magnetorheological elastomer. Dynamic elastic properties of the isolator have been presented. The stiffness of the isolator increases significantly with increasing amperage.

2) A semi-active adaptive controller has been proposed for the MRE-based isolator. The proposed controller-coupled suspension is significantly more efficient than the passive suspension.

An effective controller can be realized in the seat car suspension model using variable stiffness vibration isolators. Using the MRE model, the numerical response comes closer to the characteristics of the actual structure. In the future, we would like to carry out tests that simulate more realistic scenarios, including real-time control. The model parameters of the car seat suspension system are based on the standard model.

Acknowledgment: This research is funded by The University of Danang – University of Technology and Education under project number T2022-06-15.

REFERENCES

[1] M.R. Jolly, J.D. Carlson, B.C. Munoz, and T.A. Bullions, "The magnetoviscoelastic response of elastomer composites consisting of ferrous particles embedded in a polymer matrix", *J. Intell. Mater. Syst. Struct*, vol. 7, no. 6, pp. 613-622, 1996, https://doi.org/10.1177/1045389X9600700601.

[2] L. Chen, X.L. Gong and W.H. Li, "Microstructures and viscoelastic properties of anisotropic magnetorheological elastomers", *Smart Mater. Struct*, vol. 16, no. 6, pp. 2645–2650, 2007, DOI 10.1088/0964-1726/16/6/069.

[3] X. B. Nguyen, T. Komatsuzaki, and N. Zhang, "A nonlinear magnetorheological elastomer model based on fractional viscoelasticity, magnetic dipole interactions, and adaptive smooth Coulomb friction", *Mechanical Systems and Signal Processing*, vol. 141, Pages: 16p, 2020, https://doi.org/10.1016/j.ymssp.2019.106438.

[4] X. B. Nguyen, T. Komatsuzaki, and H. T. Truong, "Adaptive parameter identification of Bouc-wen hysteresis model for a vibration system using magnetorheological elastomer", *International Journal of Mechanical Sciences*, vol. 213, p. 106848, 2022, https://doi.org/10.1016/j.ijmecsci.2021.106848.

[5] M. Norouzi, S. M. S. Alehashem, H. Vatandoost, Y. Q. Ni, and M. M. Shahmardan, "A new approach for modeling of magnetorheological elastomers", *J. Intell. Mater. Syst. Struct*, vol. 27, no. 8, pp. 1121-1135, 2015, https://doi.org/10.1177/1045389X15615966.

[6] G. J. Liao, X. L. Gong, C. J. Kang, and S. H. Xuan, "The design of an active-adaptive tuned vibration absorber based on magnetorheological elastomer and its vibration attenuation performance", *Smart Mater Struct*, vol. 20, no. 7, pp. 5015–5025, 2011, DOI 10.1088/0964-1726/20/7/075015.

[7] W. Zhu and X. T. Rui, "Semiactive Vibration Control Using a Magnetorheological damper and a magnetorheological elastomer based on the Bouc–Wen model", *Shock. Vib*, vol. 2014, pp. 1-10, 2014, https://doi.org/10.1155/2014/405421

[8] X. B. Nguyen, T. Komatsuzaki, Y. Iwata, and H. Asanuma, "Modeling and semi-active fuzzy control of magnetorheological elastomer-based isolator for seismic response reduction", *Mech Syst Signal Process*, vol. 101, pp. 449–466, 2018, https://doi.org/10.1016/j.ymssp.2017.08.040.

[9] X. B. Nguyen, T. Komatsuzaki, Y. Iwata, and H. Asanuma, "Fuzzy Semiactive Vibration Control of Structures Using Magnetorheological Elastomer", *Shock and Vibration, Hindawi*, vol. 2017, Pages: 15p, 2012, https://doi.org/10.1155/2017/3651057.

[10] J. Fei and M. Xin, "Robust adaptive sliding mode controller for semi-active vehicle suspension system", *Int. J. Innov. Comput. Inf. Control*, vol. 8, no. 1, pp. 691–700, 2012.

[11] A. Y. Fallah and T. Taghikhany, "Sliding mode fault detection and fault tolerant control of smart dampers in semi-active control of building structures", *Smart Mater Struct*, vol. 24, no. 12, Pages: 17p, 2015, DOI 10.1088/0964-1726/24/12/125030.

[12] S. D. Nguyen, W. Kim, J. Park, and S. B. Choi, "A new fuzzy sliding mode controller for vibration control systems using integrated structure smart dampers", *Smart Mater Struct*, vol. 26, no. 4, Pages: 15p, 2017, DOI 10.1088/1361-665X/aa52fd.

[13] D. X. Phu, K. Shah, and S. B. Choi, "Design of a new adaptive fuzzy controller and its implementation for the damping force control of a magnetorheological damper", *Smart Mater Struct*, vol. 23, no. 6, Pages: 18p, 2014, DOI 10.1088/0964-1726/23/6/065012.

[14] X. B. Nguyen, T. Komatsuzaki, Y. Iwata, and H. Asanuma, "Robust adaptive controller for semi-active control of uncertain structures using a magnetorheological elastomer-based isolator", *J. Sound Vib*, vol. 434, pp. 192-212, 2018, https://doi.org/10.1016/j.jsv.2018.07.047.

[15] L. M. Jansen and S. J. Dyke, "Semi-active control strategies for MR dampers: A comparative study", *J Eng Mech*, vol. 126, no. 8, pp. 795–803, 2000, https://doi.org/10.1061/(ASCE)0733-9399(2000)126:8(795).

[16] H. T. Truong, X. B. Nguyen, and C. M. Bui, "Singularity-Free Adaptive Controller for Uncertain Hysteresis Suspension Using Magnetorheological Elastomer-Based Absorber", *Shock and Vibration*, vol. 2022, Pages: 17p, 2022, https://doi.org/10.1155/2022/2007022.

[17] X. B. Nguyen, T. Komatsuzaki, and H. T. Truong, "Novel semiactive suspension using a magnetorheological elastomer (MRE)-based absorber and adaptive neural network controller for systems with input constraints", *Mechanical Sciences*, vol. 11, no. 2, pp. 465–479, 2020, https://doi.org/10.5194/ms-11-465-2020, 2020.

[18] S. B. Choi and Y. M. Han, "Vibration control of electrorheological seat suspension with human-body model using sliding mode control", *Journal of Sound and Vibration*, vol. 30, no. 1-2, pp. 391–404, 2007, https://doi.org/10.1016/j.jsv.2007.01.027.

[19] W. Li, X. Zhang and H. Du. "Development and simulation evaluation of a magnetorheological elastomer isolator for seat vibration control", *Journal of Intelligent Material Systems and Structures*, vol. 23, no. 9, pp. 1041-1048, 2012, https://doi.org/10.1177/1045389X11435431.